J Mater Sci (2012) 47:1071–1076
DOI 10.1007/s10853-011-5896-7

Evaluation of photoanodic output on carbon cluster/phthalocyanine films with respect to the types of n-type conductors employed

Toshiyuki Abe · Kazuki Nakamura · Hiromasa Ichinohe · Keiji Nagai

Received: 31 January 2011 / Accepted: 23 August 2011 / Published online: 10 September 2011

Abstract Organic p/n bilayers, composed of carbon cluster (i.e., C_{60} or C_{70}, n-type semiconductor) and zinc phthalocyanine (denoted as ZnPc, p-type semiconductor) were prepared and used as photoelectrodes in the water phase. The bilayer (i.e., C_{60}/ZnPc or C_{70}/ZnPc) coated on a base electrode showed photoanodic characteristics in the presence of thiol, which induced the oxidation of thiol at the ZnPc/water interface along with the photophysical events (i.e., visible-light absorption, carrier generation, and its conduction) in the p/n interior. Kinetic analysis was conducted for both systems, which revealed that the overall photoelectrode reactions are kinetically dominated by the charge transfer between ZnPc and thiol. Considering the result of a reference system (i.e., a photoanode of perylene derivative/ZnPc bilayer), the photoelectrode characteristics involving the rate-limiting oxidation are discussed with respect to the types of n-type conductors.

Introduction

Development of a visible-light-responsive photodevice has attracted attention for establishing an efficient system in photoenergy conversion. Organic dye is a promising candidate for a photoexcitation center capable of visible-light absorption, which has been examined in terms of solar cells [1, 2], molecule-based photoelectrodes by means of self-assembled monolayers [3] and Langmuir-Blodgget film [4], sensitization of photocatalysts [5–7], etc. However, no such dye has been coupled with the overall decomposition of water into O_2 and H_2. Effective utilization of the organic dye may be an issue for creating a photoenergy conversion system particularly in the water phase.

Recently, we showed a novel function of organic p/n bilayer as photoelectrode in the water phase [8–15], in addition to the conventional function as photovoltaic cell in the dry state [1, 2]. That is, a photo-induced oxidation occurs at the solid (p-type semiconductor)/water interface when applying the organic p/n bilayer to a photoanode in the water phase (see Scheme 1); in addition, the inverse coating of the p/n bilayer also leads to the function as a photocathode. It appeared that such a photoelectrochemical event is associated with a series of photophysical processes (i.e., light absorption, charge separation of exciton, and carrier conduction) in the p/n interior. For example, the organic bilayer of 3,4,9,10-perylenetetracarboxyl-bisbenzimidazole (PTCBI, an n-type semiconductor)/cobalt phthalocyanine (CoPc, a p-type semiconductor) acted as a stable and efficient photoanode leading to the evolution of O_2 from water, which consequently resulted in photoelectrochemical water splitting to involve the simultaneous evolution of H_2 at the counter electrode [10]. The most advanced characteristic of the PTCBI/CoPc bilayer is that the entire visible-light energy of $\lambda < 750$ nm was available for the water oxidation at the CoPc/water interface. Few examples of such photodevices featuring an inorganic semiconductor have appeared in the literature [16, 17].

We also demonstrated the function of fullerene (denoted as C_{60}, an n-type semiconductor) as a part of the organic p/n bilayer in terms of the photoelectrode in the water phase [9, 11, 13]. Carbon clusters (such as C_{60} and C_{70})

T. Abe (✉) · K. Nakamura · H. Ichinohe
Department of Frontier Materials Chemistry,
Graduate School of Science and Technology,
Hirosaki University, 3 Bunkyo-cho, Hirosaki 036-8561, Japan
e-mail: tabe@cc.hirosaki-u.ac.jp

K. Nagai
Chemical Resources Laboratory, Tokyo Institute of Technology,
4259 Nagatsuta, Midori-ku, Yokohama 226-8503, Japan

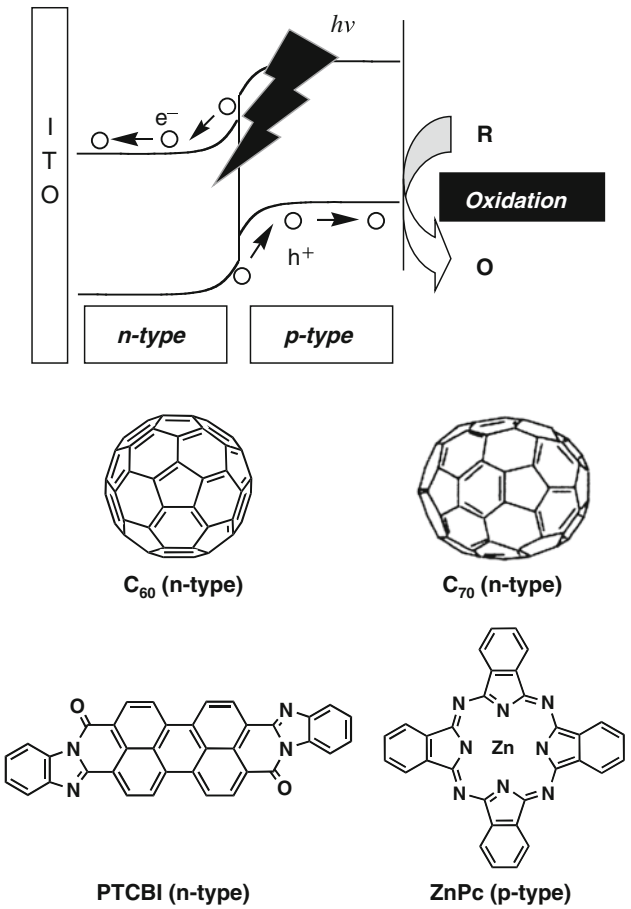

Scheme 1 Schematic illustration of organic p/n bilayer working as a photoanode in the water phase, and chemical structures of C_{60}, C_{70}, PTCBI, and ZnPc

may be key materials among the scarcity of organic n-type semiconductors because the LUMO level of organic semiconductors is usually energetically high. This study focused on the carbon clusters in the organic p/n bilayer, where those were used in combination with zinc phthalocyanine (denoted as ZnPc, a p-type semiconductor). Not only the carbon cluster/ZnPc bilayers but also the PTCBI/ZnPc bilayer were applied to photoanodes, wherein the photoelectrode kinetics was examined with respect to the types of the n-type conductors employed.

Experimental

Pure C_{60} (>99.5%) and C_{70} (>97%) were purchased from Tokyo Kasei Kogyo Co., Ltd. and Kanto Chemical Co., Inc., respectively, and used as received. PTCBI was used as a reference compound of n-type semiconductor. According to a previously described procedure [18], PTCBI was synthesized and purified. ZnPc (Kanto Chemical Co, Inc) was purified by sublimation before use, where the temperature during sublimation was maintained constant at the exterior of vessel (cf. temperature: 530 °C; degree of pressure within the vessel: ca. 2×10^{-2} Pa). 2-Mercaptoethanol was obtained from Kanto Chemical Co., Inc. The ITO-coated glass plate (sheet resistance: 8 Ω cm^{-2}; transmittance: >85%; ITO thickness: 174 nm) was from Asahi Glass Co., Ltd.

The photoelectrode device was prepared by vapor deposition (degree of pressure: ca. 5.0×10^{-4} Pa; deposition speed: 0.03 nm s^{-1}), and it comprised a carbon cluster (C_{60} or C_{70}) coated on an ITO and ZnPc coated on top of the carbon cluster layer (denoted as ITO/carbon cluster/ZnPc). The PTCBI/ZnPc bilayer was also prepared through the same procedure (denoted as ITO/PTCBI/ZnPc). During the vapor deposition, the temperature at the ITO plate was not controlled. Absorption spectral measurement was conducted using a Hitachi U-2010 spectrophotometer. The resulting absorption spectra of ZnPc [19], C_{60} [20], C_{70} [21], and PTCBI [19] were identical to those reported earlier, and their absorption coefficients indicated the thickness of the film employed (cf. the aggregation structure of ZnPc was also identifiable from the absorption spectrum; this implied that the polymorph of ZnPc is attributed to the α-phase, which is also supported by an earlier study [22]). Since it is considered that the additivity of the absorption coefficients is held in the visible-light absorption spectrum of the p/n bilayer, the two unknown parameters, i.e., the two thicknesses, were estimated by solving simultaneous equations based on absorbance at two distinct wavelengths. Such an estimation of film thickness has thus far been conducted in the cases of organic p/n bilayers [8–15]. Through the above-mentioned calculation, the typical thickness of each bilayer was estimated as 30 nm-carbon cluster and 80 nm-ZnPc for the carbon cluster/ZnPc systems, and 150 nm-PTCBI and 80 nm-ZnPc for the PTCBI/ZnPc system.

An electrochemical glass cell was equipped with a modified ITO working electrode (effective area: 1 × 1 cm), a spiral Pt counter electrode, and an Ag/AgCl (in saturated KCl electrolyte) reference electrode. The entire photoelectrochemical study was conducted in an alkaline (KOH) solution containing a known concentration of thiol within an Ar atmosphere (pH = 10). This study was conducted using a potentiostat (Hokuto Denko, HA-301) with a function generator (Hokuto Denko, HB-104), a coulomb meter (Hokuto Denko, HF-201), and an X–Y recorder (GRAPHTEC, WX-4000) under illumination. A halogen lamp (light intensity: ca. 100 mW cm^{-2}) was used as the light source under typical conditions. While measuring the action spectrum for photocurrent, a halogen lamp was used as the light source in combination with a monochromator (Soma Optics, Ltd., S-10). Light intensity was measured using a power meter (type 3A from Ophir Japan, Ltd.). The incident photon-to-current conversion efficiency (denoted as IPCE) was calculated by the following equation:

$$\mathrm{IPCE}(\%) = ([I/e]/[W/\varepsilon]) \times 100 \quad (1)$$

where I (A cm^{-2}) is the photocurrent density; e (C), the elementary electric charge; W (W cm^{-2}), the light intensity; and ε, the photon energy. In this study, the effect of the reflection of the incident light from the glass surface was not considered (i.e., the light intensity was not corrected).

Results and discussion

Figure 1 shows the cyclic voltammograms measured at the ITO/carbon cluster/ZnPc (i.e., ITO/C_{60}/ZnPc and ITO/C_{70}/ZnPc). In both systems, the generation of photoanodic currents was found to involve the oxidation of thiol; while, no response was observed in the dark. These findings are consistent with typical photoelectrochemical characteristics occurring at a phthalocyanine surface in organic p/n bilayer [8, 10–13, 15]; that is, the photoanodic currents generated at the ZnPc/water interfaces are attributed to carrier generation at the p/n interfaces and the following event of hole conduction through the ZnPc layer. The detailed mechanism is discussed later. Figure 1 also reveals that ITO/C_{70}/ZnPc can show the similar characteristics to ITO/C_{60}/ZnPc under illumination and in the dark.

In order to determine the origin of the photoanodic currents generated at the ITO/carbon cluster/ZnPc, in each system the action spectrum for photocurrent was measured and then compared with the absorption spectrum of the bilayer employed. When irradiation was conducted from the side of carbon cluster (Fig. 2a), in each case the photocurrent occurred over the entire visible-light region of $\lambda < 750$ nm; while, in the cases where monochromatic light was irradiated from the ZnPc side (Fig. 2b), the resulting action spectra were almost in agreement with a transmittance spectrum of ZnPc (Fig. 2b). In summary, in each case the action spectrum was inconsistent with the absorption spectrum of the carbon cluster/ZnPc bilayer (Fig. 2c), thereby showing that the photoanodic current generation cannot be induced on the visible-light absorption over the whole bilayer. Considering that despite little presence of the absorption of ZnPc at around 400–500 nm

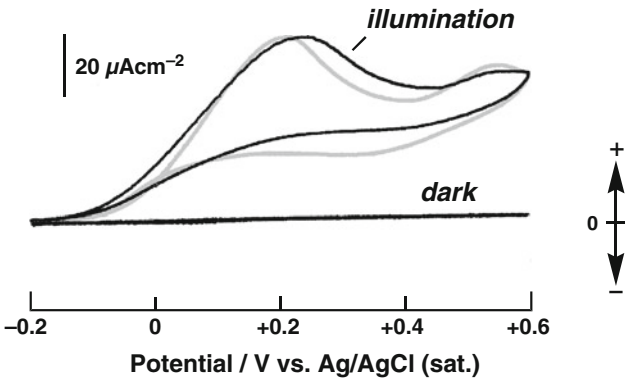

Fig. 1 Cyclic voltammograms at ITO/C_{60}/ZnPc (*solid line*) and ITO/C_{70}/ZnPc (*gray line*). In the dark, the voltammograms of both systems overlapped each other. Irradiation was conducted from the ITO side. Concentration of thiol, 1.0×10^{-3} mol dm^{-3} (pH = 10); film thickness of bilayer, 25 nm (C_{60} or C_{70})/80 nm (ZnPc); light intensity = 100 mW cm^{-2}; scan rate = 20 mV s^{-1}

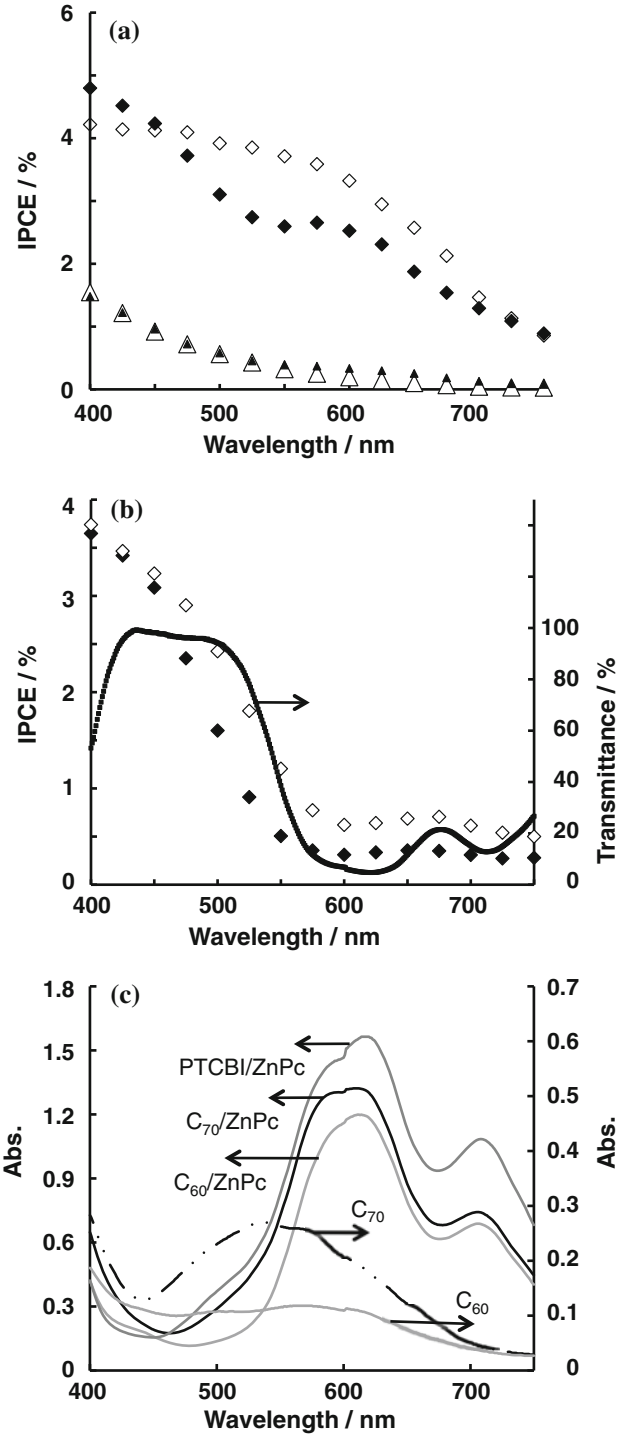

◀ **Fig. 2** **a** Action spectra for photocurrents generated at ITO/C_{60}/ZnPc (*filled diamond*), ITO/C_{70}/ZnPc (*unfilled diamond*), ITO/C_{60} (*filled triangle*), and ITO/C_{70} (*unfilled triangle*). Concentration of thiol, 1.0×10^{-3} mol dm^{-3} (pH = 10); film thickness, 30 nm (C_{60} or C_{70})/80 nm (ZnPc); film thickness, 30 nm (single layer of C_{60} or C_{70}); applied potential, +0.3 V; irradiation direction of the incident light, the side of carbon cluster. **b** Action spectra for photocurrents generated at ITO/C_{60}/ZnPc (*filled diamond*) and ITO/C_{70}/ZnPc (*unfilled diamond*), and a transmittance spectrum of the single-layered ZnPc. Concentration of thiol, 1.0×10^{-3} mol dm^{-3} (pH = 10); film thickness, 30 nm (C_{60} or C_{70})/80 nm (ZnPc); applied potential, +0.3 V; irradiation direction of the incident light, the side of ZnPc. **c** Absorption spectra of the bilayers employed and the single-layered carbon clusters

(see Fig. 2b), the photocurrent generation was confirmed, it may mean that the photoanodic currents at the ZnPc/water interfaces originate in the wide visible-light absorption by only the carbon clusters (see Fig. 2c); however, the action spectrum of the single-layered carbon cluster (i.e., ITO/C_{60} or ITO/C_{70}) was different from that of the corresponding bilayer in terms of magnitude and spectral shape (see Fig. 2a). Therefore, the results of Fig. 2 suggest that an absorption of ZnPc probably close to the p/n interface can also contribute to the photocurrent generation.

The mechanism of the present photocurrent generation is described as follows: the carbon cluster and ZnPc absorb visible light, through which excitons are formed. The excitons are considered to be separated at the p/n interfaces. In order to estimate a photovoltage of each carbon cluster/ZnPc system, the rest potentials at single-layered C_{60}, C_{70}, and ZnPc were measured under illumination (in an alkaline solution containing 1×10^{-3} mol dm^{-3} of thiol), according to a previously reported procedure [12, 23]. The rest potentials of carbon clusters were less positive than that of ZnPc (cf. rest potential (V vs. Ag/AgCl): C_{60}, −0.32 V; C_{70}, −0.35 V; ZnPc, −0.04 V), and thus, the differences are consistent with the photovoltage generated in the carbon cluster/ZnPc systems. The presence of photovoltage (i.e., for C_{60}/ZnPc system, 280 mV; for C_{70}/ZnPc system, 310 mV) supports the formation of built-in-potential at the p/n interfaces. After charge separation at the p/n interfaces, the photogenerated carriers of C_{60}^{-} (or C_{70}^{-}) and $ZnPc^{+}$ migrate in each layer, and thus, ZnPc has oxidizing power for the thiol oxidation at the solid/water interface (i.e., $ZnPc^{+} + RS^{-} \rightarrow ZnPc + RS^{\bullet -}$) [12].

The time course of photocurrent was measured to evaluate the kinetic characteristics of both ITO/C_{60}/ZnPc and ITO/C_{70}/ZnPc. Typical examples are shown in Fig. 3. In each system, a spiky photocurrent (J_{in}) was initially observed, after which it attained a steady state (J_s represents a steady-state photocurrent). Such a photoelectrochemical response is usually characterized by the rate-limiting charge transfer at the solid/water interface. In both systems, the photoelectrode characteristics were investigated with

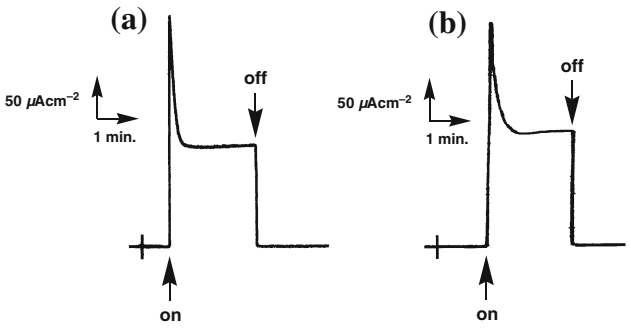

Fig. 3 Transient photocurrents generated at **a** ITO/C_{60}/ZnPc and **b** ITO/C_{70}/ZnPc immediately after irradiation with white light (intensity, 100 mW cm^{-2}). Irradiation was conducted from the ITO side. Concentration of thiol, 3.0×10^{-3} mol dm^{-3} (pH = 10); film thickness, 30 nm (C_{60} or C_{70})/80 nm (ZnPc); applied potential, +0.3 V

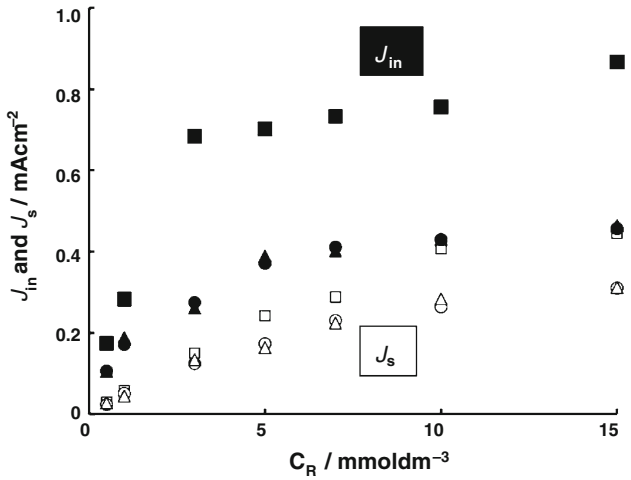

Fig. 4 The dependencies of initial spiky photocurrent (J_{in}, *filled circle*: ITO/C_{60}/ZnPc; *filled triangle*: ITO/C_{70}/ZnPc; *filled square*: ITO/PTCBI/ZnPc) as well as steady-state photocurrent (J_s, *unfilled circle*: ITO/C_{60}/ZnPc; *unfilled triangle*: ITO/C_{70}/ZnPc; *unfilled square*: ITO/PTCBI/ZnPc) on the thiol concentrations. Film thickness, 30 nm (C_{60} or C_{70})/80 nm (ZnPc); film thickness, 150 nm (PTCBI)/80 nm (ZnPc); light intensity = 100 mW cm^{-2}; applied potential = +0.3 V

respect to the concentration of thiol (see Fig. 4). In a reference study, the PTCBI/ZnPc bilayer (see Fig. 2), which has been identified as a photoanode by the authors [12], was also investigated under the similar experimental conditions [i.e., applied potential, electrolyte solution, and the magnitude of visible-light absorption particularly in the region of $\lambda < \sim 500$ nm (cf. there was a little or no contribution of the absorption of ZnPc to the generation of photoanodic currents)]. In all cases studied, the resulting photocurrents exhibited the same response as shown in Fig. 3. Saturation in the concentration was observed for both J_{in} and J_s,

implying that the photo-induced oxidation at the ZnPc/water interface is not kinetically controlled by the mass transfer of thiol (i.e., diffusion). Furthermore, it should also be noted from Fig. 4 that, particularly irrespective of the types of carbon clusters, the resulting J_{in} and J_s showed a similar dependence on the thiol concentration.

Based on the above-mentioned results, the two types of photocurrent (J_{in} and J_s) were analyzed to assume an adsorption step before the rate-limiting charge transfer step, wherein a model was applied to the present kinetic analysis (i.e., the Langmuir adsorption equilibrium for thiol at the ZnPc surface was assumed) [12, 24]. In the present case, the photocurrent (J) is assumed to be proportional to the surface concentrations of holes ($[h^*]_0$) as well as of the adsorbed thiol (Γ), and is represented as

$$J/nF = k_f[h^*]_0\Gamma \quad (2)$$

where n is the number of electrons transferred from a thiol to ZnPc (in the present case, $n = 1$), F is Faraday's constant, and k_f is the rate constant of the electrochemical reaction between thiol and ZnPc. The kinetic analyses of J_{in} and J_s were conducted using

$$C_R/J_{in} = C_R/J_{max} + (k'/k)/J_{max} \quad (3)$$

$$C_R/J_s = C_R/J_{max} + \left\{(k'/k) + \left(k_f[h^*]_0/k\right)\right\}/J_{max} \quad (4)$$

where k is the rate constant of adsorption at ZnPc (bimolecular process), k' is the rate constant of desorption (monomolecular process), C_R is the thiol concentration in the electrolyte solution, and J_{max} is the postulated photocurrent with maximum coverage occupying all available sites.

By applying the data of Fig. 4 to the Eqs. 3 and 4, kinetic analysis was conducted for each system. It was confirmed through the analyses that the application of the present model is valid, and thus, the kinetic parameters of J_{max}, k'/k, and $k_f[h^*]_0/k$ were obtained (Table 1). The analysis results revealed that the parameters are independent of the types of carbon clusters employed. As for the inverse of the k'/k term [i.e., k/k' (=equilibrium constant for adsorption (K))], in all the systems it resembles each other; this is reasonable because the K values correspond to the net adsorption rate of thiol at the ZnPc surface. The $k_f[h^*]_0/k$ term, representative of the effectiveness of the ZnPc/water interfaces for the rate-limiting oxidation, is larger in the PTCBI/ZnPc system than in the carbon cluster/ZnPc systems. Based on the definition of the kinetic parameters, the $k_f[h^*]_0/k$ values in the carbon cluster/ZnPc systems are also indicative of constant $[h^*]_0$; in other words, the influence of kinetically fast processes in the p/n interior may be incorporated into the constant concentration of $[h^*]_0$, which is independent of the types of carbon clusters. The kinetic analysis also indicates a high value of $[h^*]_0$ in the PTCBI/ZnPc system; this explicitly affects the value of J_{max} because the J_{max} term is proportional to $[h^*]_0$ as well as Γ (cf. constant in each system) at the ZnPc/water interface (see Eq. 2). The present result shows that PTCBI acts as an efficient n-type conductor in the photoanode of organic p/n bilayer; particularly in the PTCBI/ZnPc system, an efficient charge separation may take place at the p/n interface, thus leading to a high output at the ZnPc surface.

Conclusion

The photoelectrode characteristics of organic p/n bilayer in the water phase were examined with the types of n-type conductors, for which the photoanodes composed of an n-type conductor (i.e., C_{60}, C_{70}, or PTCBI) and p-type ZnPc were prepared. In addition to the PTCBI/ZnPc bilayer [12], the carbon cluster/ZnPc bilayers were also found to work as photoanodes responsive to a wide visible-light energy. On kinetic aspects, the systems employed were dominated by charge transfer at the ZnPc/water interface (cf. in solar cells in the dry state, the rate-determining step is the carrier generation at p/n interface [21]); moreover, the magnitude of the kinetics at the ZnPc/water interface was independent of the types of carbon clusters, which also involved that the steady concentration of the hole ($[h^*]_0$) available for the rate-limiting oxidation is constant in each system; in addition, the higher value of $[h^*]_0$ in the PTCBI/ZnPc system appeared to result in an efficient output, probably due to an efficient charge separation at the p/n interface. Although the energy levels of the conduction band (CB) and valence band (VB) in carbon clusters (cf. C_{60}: CB = 6.2 eV, VB, 4.5 eV [25]; C_{70}: CB = 6.4 eV, VB = 4.3 eV [26]) are similar to those in PTCBI (cf. CB = 6.2 eV, VB = 4.5 eV [27]), the present analyses revealed the kinetic characteristics of the rate-limiting oxidation at the ZnPc surface featuring n-type conductors. The improvement of $[h^*]_0$ will result in a high

Table 1 The resulting kinetic parameters of ITO/C_{60}/ZnPc, ITO/C_{70}/ZnPc, and ITO/PTCBI/ZnPc

Systems	J_{max} (from J_{in}), μA cm^{-2}	J_{max} (from J_s), μA cm^{-2}	k'/k, mol dm^{-3}	K, (mol dm^{-3})$^{-1}$	$k_f[h^*]_0/k$, mol dm^{-3}
ITO/C_{70}/ZnPc	5.28×10^2	5.27×10^2	2.17×10^{-3}	4.61×10^2	7.55×10^{-3}
ITO/C_{60}/ZnPc	5.23×10^2	5.20×10^2	2.14×10^{-3}	4.68×10^2	7.55×10^{-3}
ITO/PTCBI/ZnPc	9.68×10^2	9.22×10^2	2.09×10^{-3}	4.79×10^2	1.28×10^{-2}

efficiency of organic p/n bilayers in the water phase. Making the uses of the great variety of types of organic semiconductors and its easy processing, further design and development of organic photoelectrodes is a future issue to be addressed.

References

1. Tang CW (1986) Appl Phys Lett 48:183
2. Yang F, Shtein M, Forrest SR (2005) Nat Mater 4:37
3. Uosaki K, Kondo T, Zhang XQ, Yanagida M (1997) J Am Chem Soc 119:8367
4. Wu DG, Huang CH, Gan LB, Zheng J, Huang YY, Zhang W (1999) Langmuir 15:7276
5. Shimidzu T, Iyoda T, Koide Y (1985) J Am Chem Soc 107:35
6. Abe R, Sayama K, Arakawa H (2002) Chem Phys Lett 362:441
7. Li Q, Jin Z, Peng Z, Li Y, Li S, Lu G (2007) J Phys Chem C 111:8237
8. Abe T, Nagai K, Kaneko M, Okubo T, Sekimoto K, Tajiri A, Norimatsu T (2004) ChemPhysChem 5:716
9. Abe T, Nagai K, Sekimoto K, Tajiri A, Norimatsu T (2005) Electrochem Commun 7:1129
10. Abe T, Nagai K, Kabutomori S, Kaneko M, Tajiri A, Norimatsu T (2006) Angew Chem Int Ed 45:2778
11. Abe T, Nagai K, Ichinohe H, Shibata T, Tajiri A, Norimatsu T (2007) J Electroanal Chem 599:65
12. Abe T, Miyakushi S, Nagai K, Norimatsu T (2008) Phys Chem Chem Phys 10:1562
13. Abe T, Tobinai S, Nagai K (2009) Jpn J Appl Phys 48:021503
14. Abe T, Kamei Y, Nagai K (2010) Solid State Sci 12:1136
15. Abe T, Ichinohe H, Kakuta S, Nagai K (2010) Jpn J Appl Phys 49:015101
16. Nazeeruddin MdK, Péchy P, Grätzel M (1997) Chem Commun 1705
17. Wang ZS, Yamaguchi T, Sugihara H, Arakawa H (2005) Langmuir 21:4272
18. Maki T, Hashimoto H (1952) Bull Chem Soc Jpn 25:411
19. Morikawa T, Adachi C, Tsutsui T, Saito S (1990) Nippon Kagaku Kaishi 962
20. Capobianchi A, Tucci M (2004) Thin Solid Films 451–452:33
21. Pfuetzner S, Meiss J, Petrich A, Riede N, Leo K (2009) Appl Phys Lett 94:223307
22. Yoshida H, Tokura Y, Koda T (1986) Chem Phys 109:375
23. Oekermann T, Schlettwein D, Wöhrle D (1997) J Appl Electrochem 27:1172
24. Kermann E, Schlettwein D, Jaeger NI (1996) J Electroanal Chem 405:149
25. Peumans P, Forrest SR (2001) Appl Phys Lett 79:126
26. Rand BP, Burk DP, Forrest SR (2007) Phys Rev B 75:115327
27. Peumans P, Bulovíc V, Forrest SR (2000) Appl Phys Lett 76:2650